Static and free vibration analysis of laminated beams by refined theory based on Chebyshev Polynomials

Static and free vibration analysis of laminated beams by refined theory based on Chebyshev Polynomials

M. Filippi[*], A. Pagani[†], M. Petrolo[‡], G. Colonna[§], E. Carrera[¶]

Department of Mechanical and Aerospace Engineering, Politecnico di Torino,
Corso Duca degli Abruzzi 24, 10129 Torino, Italy.

Accepted Manuscript

Author for correspondence:
E. Carrera, Professor of Aerospace Structures and Aeroelasticity,
Department of Mechanical and Aerospace Engineering,
Politecnico di Torino,
Corso Duca degli Abruzzi 24,
10129 Torino, Italy,
tel: +39 011 090 6836,
fax: +39 011 090 6899,
e-mail: erasmo.carrera@polito.it

[*]Research Fellow, e-mail: matteo.filippi@polito.it
[†]Research Fellow, e-mail: alfonso.pagani@polito.it
[‡]Research Fellow, e-mail: marco.petrolo@polito.it
[§]Graduate student, e-mail: giovanni.colonna@polito.it
[¶]Professor of Aerospace Structures and Aeroelasticity, e-mail: erasmo.carrera@polito.it

Abstract

This paper presents a new class of refined beam theories for static and dynamic analysis of composite structures. These beam models are obtained by implementing higher-order expansions of Chebyshev polynomials for the three components of the displacement field over the beam cross-section. The Carrera Unified Formulation (CUF) is adopted to obtain higher-order beam models. The governing equations are written in terms of fundamental nuclei, which are independent of the choice of the expansion order and the interpolating polynomials. Static and free vibration analysis of laminated beams and thin walled boxes has been carried out. Results obtained with the novel Chebyshev Expansion (CE) model have been compared with those available in the literature. For comparison, Taylor-like Expansion (TE) and Lagrange Expansion (LE) CUF models, commercial codes, analytical and experimental data are exploited. The performances of refined beam models in terms of computational cost and accuracy in comparison to the reference solutions have been assessed. The analysis performed has pointed out the high level of accuracy reached by the refined beam models with lower computational costs than 2D and 3D Finite Elements.

Keywords: Refined beam theories, Finite Elements, Carrera unified formulation, laminated beams, 2D Chebyshev polynomials.

1 Introduction

One-dimensional (1D) theories have wide applications in several engineering fields. The analysis of slender, isotropic, homogeneous solid-section structures subject to bending can be often performed by means of classical beam theories. Therefore, the Euler-Bernoulli Beam Theory (EBBT) [1] or Timoshenko Beam Theory (TBT) [2, 3] are often adopted. Their low computational cost provides a powerful tool for structural analysis, although their reliability strongly depends on the preliminary assumptions adopted. For example, both models yield to poor results whenever thin walled and composite beams are considered or non-classical effects are involved. Composite and laminated structures have extended their field of application due to their attractive properties. The analysis of composite structures requires analysis tools capable to consider their complex behaviour. In most cases, burdensome three-dimensional (3D) finite elements are needed to obtain reliable results with the desired level of accuracy. In order to circumvent the problem, several refined 1D or 2D theories have been developed over the years. These theories are aimed to maintain the simplicity and the low computational cost of beam models but are capable to detect non-classical phenomena with the desired level of accuracy. Khdeir [4] [5] [6] used the theory developed by Reddy [7] to provide exact solutions for static and dynamic analysis of cross-ply laminated beams. Moreover, Surana [8] presented a 2-D curved beam element, using Lagrange's polynomials to obtain higher-order models. Rao [9] used Taylor series expansions to include the displacement components in the cross-section plane. The generalized Timoshenko theory for composite beams embedded in the Variational Asymptotic Method was used in [10] for the calculation of sectional stiffness and shear center location for composite beam buckling and free vibration analyses. A closed-form solution for the detection cross-section warping phenomena has been proposed in [11], whereas two different 1D FE elements were presented in [12], with enriched axial and transverse displacement fields. Karama [13] addressed his studies on composite beams, considering exponential functions to ensure the continuity of shear stresses. Dynamic and static analyses were performed on laminated beams in [14, 15]. The dynamic stiffness method (DSM) was used in [16] to improve the prediction of flexural frequencies of laminated beams. In particular, the first-order shear deformation theory was used to take into account the important shear effects that occur in this type of structure. Li [17] used the DSM and a trigonometric shear deformation theory for laminated beams. Moreover, Piovan [18] and Mitra et al. [19] introduced theories capable to take into account the shear deformability. These models could deal with beams with arbitrary cross-section with open or closed contour. In more recent works, Vidal [20] approximated the displacement field as a sum of separate functions of the axial and the transverse coordinate. Mantari [21] expressed the displacement components in laminated as a combination of exponential and trigonometric terms. In [22], the stability and the static behaviour of laminated beams with inverse hyperbolic shear deformation was studied. Shimpi [23] presented a trigonometric layer-wise model for two-layered cross-ply beams, whereas Tahani [24] developed two different theories for laminated beam static and dynamic analysis. The first consists of adapting the layer-wise theory for plates to beams, the second developed a beam theory following a procedure similar to those adopted for

plates and shells. As the number of layers increases, the use of the layer-wise approach is limited by the increase in computational cost. Hence, layer independent theories have been developed, using Heaviside's or zig-zag functions. Murakami [25] introduced a zig-zag function into Reissner's new mixed variational principle. In [26], a refined sine model with Heaviside function for each layer was presented, whereas the sine model was improved by introducing Murakami's function in [27]. Onate [28] introduced a new linear two-node beam element based on the combination of Timoshenko and refined zig-zag kinematics. Further studies have been made in [29] and [30] aimed to develop a general and reliable theory capable to capture every aspect of the complex nature of the composite materials.

The refined beam theories used in the present work have been developed in the framework of the Carrera Unified Formulation. The CUF has been developed for plates and shell analysis [31, 32]. Over the last years, the CUF has been extended to beam structures [33, 34]. The unique feature of CUF models is due to their hierarchical formulation, which enables the arbitrary choice of the expansion functions over the cross-section up to the desired order. Any-order structural model can be therefore implemented with no need for formal changes in the problem equations and matrices. The use of a CUF model allows us to deal with arbitrary geometries, boundary conditions and material configurations with no need for ad hoc formulation. CUF capabilities combined with the simplicity of 1D models allow us to detect shell and solid like solutions for either static [35], free-vibration [36, 37] and buckling [38, 39] analyses by means of the Taylor-like Expansion (TE). In [34], the contribution of each higher-order term to the final solution has been evaluated. Structural models included thin-walled sections, point loads and shell-like natural modes, whereas further studies have been addressed towards the analysis of open cross-sections, lateral edge enforced boundary conditions and layer-wise approaches [40]. Moreover, in [40] the displacement field across the section was modeled by means of Lagrange polynomials, whereas in [41] trigonometric, exponential and zig-zag theories have been used. Lagrange Expansion (LE) models used in [42] for the analysis of laminated anisotropic composites via the component-wise approach have the great advantage of considering only pure displacement variables.

In the present paper, the bi-dimensional Chebyshev polynomials of the second kind have been used in the framework of the Carrera Unified Formulation (CUF) to develop a novel refined beam theory. Chebyshev Polynomials have been widely used in solving differential equations and eigenvalue problems due to their fast convergence. For example, Zhou et al. [43, 44] used Chebyshev polynomials in studying the three-dimensional vibration of thick rectangular and circular plates. Also, Sinha and Butcher [45, 46] used Chebyshev polynomials to study the stability of systems with parametric excitation and structures with time-dependent loads. Nath and Kumar proposed a methodology based on approximating the space in double Chebyshev series to analyze the non-linear behaviour of rectangular plates [47]. In [48], the effects of non-ideal boundary conditions on the natural frequencies of beams and columns with variable cross-section subject to follower forces were investigated. Moreover, Ruta [49] dealt with linear vibrations of the Timoshenko beam with variable strength and geometric parameters. Functions that described the beams variable parameters (i.e. flexural

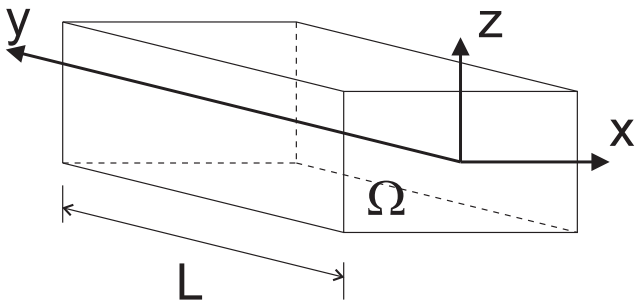

Figure 1: Coordinate frame of the beam.

rigidity, density, variable foundation parameters and loads) were implemented. These functions were then expanded into convergent series relative to Chebyshev polynomials of the first kind.

In this work, static and free vibration analysis of an Aluminum alloy box made has been carried out. Subsequently the static and dynamic analysis of laminated, sandwich and composite beams has been carried out. The results have been compared with those obtained from TE and LE CUF theories, commercial FEM code analyses, experimental and analytical data. In the present paper, Section 2 gives an overview of the Classical Beam Theories, whereas in Section 3 the higher-order beam theories developed in the framework of CUF are presented. Moreover, the Chebyshev Expansion beam theories are introduced in Section 4. In Section 5, a brief outline of the FEM approach is given, whereas Section 6 is devoted to the presentation of the results obtained by the novel CE approach. Conclusions are drawn in Section 7

2 Classical beam theories

The Cartesian coordinate system adopted for a generic beam is shown in Fig. 1. Although the cross-section reported in the figure is rectangular, the validity of the proposed formulation is not affected by this choice, which is adopted for merely illustrative purpose. According to Euler-Bernoulli Beam Theory (EBBT), the kinematic field is

$$\begin{aligned} u(x,y,z) &= u_1(y) \\ v(x,y,z) &= v_1(y) - x\,\frac{\partial u_1(y)}{\partial y} + z\,\frac{\partial w_1(y)}{\partial y} \\ w(x,y,z) &= w_1(y) \end{aligned} \tag{1}$$

where u, v and w are the displacement components of a point along x, y and z axes, respectively; u_1, v_1 and w_1 are the displacements of the beam axis, whereas $-\dfrac{\partial u_1}{\partial y}$ and $\dfrac{\partial w_1}{\partial y}$ are the rotations of the cross-section about the z-axis (i.e. ϕ_z) and x-axis (i.e. ϕ_x). In EBBT, since the cross-sectional shear deformation phenomena are neglected, the deformed cross-section is assumed plane and orthogonal to the beam axis. However, several problems (e.g., short beams and composite structures) require the inclusion of shear stresses since their neglect can lead to incorrect results. It is, therefore, necessary to generalize Eq. (1) and overcome the assumption of the orthogonality of the cross-section. The Timoshenko Beam Theory (TBT) provides an

enhanced displacement field

$$\begin{aligned} u(x,y,z) &= u_1(y) \\ v(x,y,z) &= v_1(y) - x\ \phi_z(y) - z\ \phi_x(y) \\ w(x,y,z) &= w_1(y) \end{aligned} \tag{2}$$

It is clear that TBT constitutes an improvement over EBBT. In fact, the cross-section does not necessarily remain perpendicular to the beam axis after deformation. Moreover, the original displacement field is enriched by two degrees of freedom (i.e. the unknown rotations, ϕ_z and ϕ_x).

3 Higher-order, hierarchical models by CUF

Classical beam models provide a reasonably good approximation of slender, solid section and homogeneous structures subjected to bending loads. However, in the case of short, thin-walled, open cross-section beam analysis the required degree of accuracy may not be reached. In this case, more sophisticated theories, which adopt richer kinematic fields to obtain more accurate 1D models, are needed. By means of the Carrera Unified Formulation (CUF), refined beam models with an arbitrary number of terms in the kinematic field can be developed. The kinematics of a CUF beam model can be summarized as follows:

$$\mathbf{u}(x,y,z) = F_\tau(x,z)\mathbf{u}_\tau(y), \qquad \tau = 1,2,....,M \tag{3}$$

where F_τ indicates the functions of the cross-section coordinates x and z, $\mathbf{u}_\tau$ is the generalized displacement vector and M indicates the number of terms in the expansion. Since the generalized Einstein notation has been adopted, the repeated subscript indicates summation. The choice of F_τ and the number of terms M are arbitrary. The models known from the literature as TE [33, 50, 51] are obtained considering the Taylor-like polynomials as F_τ functions. It should be noted that Eq. (1) and (2) are particular cases of the linear ($N = 1$) TE model, which can be expressed as:

$$\begin{aligned} u(x,y,z) &= u_1(y) + x\ u_2(y) + z\ u_3(y) \\ v(x,y,z) &= v_1(y) + x\ v_2(y) + z\ v_3(y) \\ w(x,y,z) &= w_1(y) + x\ w_2(y) + z\ w_3(y) \end{aligned} \tag{4}$$

where the parameters on the right-hand side (u_1, v_1, w_1, u_2, etc.) represent linear displacements and rotations of the beam axis. Higher-order generalized displacements can be automatically included as the order N is increased. More details about TE models and the formulation of classical models as particular cases of TE can be found in [52, 53].

4 CUF models based on Chebyshev polynomials

4.1 $1D$ Chebyshev polynomials

Chebyshev Polynomials (CP) are generally divided into two classes. The first one is given by:

$$\begin{aligned} &T_n(x) : \mathbb{R} \Rightarrow \mathbb{C} \\ &T_n(x) = \cos n\theta \end{aligned} \tag{5}$$

n being a non negative integer, and is called Chebyshev polynomial of degree n of the *first kind*. The second one is given by:

$$\begin{aligned} &U_n(x) : \mathbb{R} \Rightarrow \mathbb{C} \\ &U_n(x) = \frac{\sin(n+1)\theta}{\sin\theta} \end{aligned} \tag{6}$$

and is called CP of degree n of the *second kind*. The polynomials of the first kind are the mathematical solutions of the Chebyshev differential equation:

$$(1-x^2)y'' - xy' + n^2 y = 0 \tag{7}$$

They can be recursively generated with the following formula:

$$\begin{aligned} T_0(x) &= 1 \\ T_1(x) &= x \\ T_2(x) &= 2x^2 - 1 \\ T_3(x) &= 4x^3 - 3x \\ T_4(x) &= 8x^4 - 8x^2 + 1 \\ T_5(x) &= 16x^5 - 20x^3 + 5x \\ T_{n+1}(x) &= 2xT_n(x) - T_{n-1}(x) \end{aligned} \tag{8}$$

CP are ortogonal with respect to the weight function $W(x) = \frac{1}{\sqrt{1-x^2}}$ and valid over the interval [-1,1]. Furthermore, the CP zeros can be defined in [-1,1] as follows:

$$x_i = (\tfrac{(2i-1)\pi}{2n}) \qquad \text{i=1..n} \tag{9}$$

Polynomials $P_n^{-1/2}(x)$ and $P_n^{1/2}(x)$ have been defined in [54]. Given the field $\mathbb{C}$ and $n \geq 0$, these polynomials are closely related to the classical CP, because

$$P_n^{-1/2}(2\cos\theta) = 2T_n(\cos\theta) \qquad \text{and} \quad P_n^{1/2}(2\cos\theta) = U_n(\cos\theta) \tag{10}$$

Considering $u = e^{i\theta}$:

$$P_n^{-1/2}(2x) = 2T_n(x) \qquad \text{and} \quad P_n^{1/2}(2x) = U_n(x) \tag{11}$$

4.2 $2D$ Chebyshev polynomials

Classical CPs have been extended over a bi-dimensional field in [54]. Polynomials $P_{m,n}^{-1/2}(x,z)$ are defined as a generalization of the CP of the first kind. On the other hand, $P_{m,n}^{1/2}(x,z)$ can be considered as a generalization of the polynomials of the second kind. For the sake of brevity, the mathematical procedure to derive both classes of polynomials has been omitted. A more detailed explanation can be found in [54] and [55]. Each polynomial of the first kind having m, n above 2 can be obtained using one of the *recurrence relations*:

$$\begin{aligned} P_{m,n}^{-1/2}(x,z) &= x \cdot P_{m-1,n}^{-1/2} - z \cdot P_{m-2,n}^{-1/2} + P_{m-3,n}^{-1/2} \\ P_{m,n}^{-1/2}(x,z) &= z \cdot P_{m,n-1}^{-1/2} - x \cdot P_{m,n-2}^{-1/2} + P_{m,n-3}^{-1/2} \end{aligned} \tag{12}$$

For m, n up to 2 the following relations hold:

$$\begin{aligned} P_{0,0}^{-1/2}(x,z) &= 6 \\ P_{1,0}^{-1/2}(x,z) &= 2x \\ P_{1,1}^{-1/2}(x,z) &= xz - 3 \\ P_{2,0}^{-1/2}(x,z) &= 2x^2 - 4z \\ P_{2,1}^{-1/2}(x,z) &= x^2 z - 2z^2 - x \\ P_{2,2}^{-1/2}(x,z) &= x^2 z^2 - 2x^3 - 2z^3 + 4xz - 3 \end{aligned} \tag{13}$$

Moreover, the $2D$ polynomials of the second kind having m, n above 2 can be obtained using again one of the following *recurrence relations*:

$$\begin{aligned} P_{m,n}^{1/2}(x,z) &= x \cdot P_{m-1,n}^{1/2} - z \cdot P_{m-2,n}^{1/2} + P_{m-3,n}^{1/2} \\ P_{m,n}^{1/2}(x,z) &= z \cdot P_{m,n-1}^{1/2} - x \cdot P_{m,n-2}^{1/2} + P_{m,n-3}^{1/2} \end{aligned} \tag{14}$$

For m, n up to 2 the following relations hold:

$$\begin{aligned} P_{0,0}^{1/2}(x,z) &= 1 \\ P_{1,0}^{1/2}(x,z) &= x \\ P_{1,1}^{1/2}(x,z) &= xz - 1 \\ P_{2,0}^{1/2}(x,z) &= x^2 - z \\ P_{2,1}^{1/2}(x,z) &= x^2 y - z^2 - x \\ P_{2,2}^{1/2}(x,z) &= x^2 z^2 - x^3 - z^3 \end{aligned} \tag{15}$$

4.3 Chebyshev Expansion Models (CE)

In the present work, Chebyshev $2D$ Polynomials of the second kind have been used as F_τ in the framework of CUF. For example, by means of the hierarchical procedure introduced by CUF, the CE second-order kinematic model with 18 generalized displacement variables can be defined as follows:

$$\begin{aligned}
u(x,y,z) &= P_{00}(x,z)u_1(y) + P_{10}(x,z)u_2(y) + P_{01}(x,z)u_3(y) + P_{20}(x,z)u_4(y) + P_{11}(x,z)u_5(y) + P_{02}(x,z)u_6(y) \\
v(x,y,z) &= P_{00}(x,z)v_1(y) + P_{10}(x,z)v_2(y) + P_{01}(x,z)v_3(y) + P_{20}(x,z)v_4(y) + P_{11}(x,z)v_5(y) + P_{02}(x,z)v_6(y) \\
w(x,y,z) &= P_{00}(x,z)w_1(y) + P_{10}(x,z)w_2(y) + P_{01}(x,z)w_3(y) + P_{20}(x,z)w_4(y) + P_{11}(x,z)w_5(y) + P_{02}(x,z)w_6(y)
\end{aligned} \tag{16}$$

The above model is analogous to the second-order TE model since it involves three constant variables, six linear and nine parabolic terms. More refined CE models can be straightforwardly formulated by hierarchically enriching the kinematics above with higher-order CP. The present work will consider only full models, in which every term of the N-order expansion is taken into account.

5 Finite element formulation

5.1 Geometrical and constitutive relations

Let us adopt the reference system chosen in Fig. 1, in which the cross-section Ω is normal to the beam axis y, which has boundaries $0 \leq y \leq L$. The stress σ and the strain ϵ components are defined as follows:

$$\begin{aligned}
\sigma &= \{\sigma_{yy}, \sigma_{xx}, \sigma_{zz}, \sigma_{xz}, \sigma_{yz}, \sigma_{xy}\}^T \\
\epsilon &= \{\epsilon_{yy}, \epsilon_{xx}, \epsilon_{zz}\epsilon_{xz}, \epsilon_{yz}, \epsilon_{xy}\}^T
\end{aligned} \tag{17}$$

In case of small displacements, that is linear behavior, the following relation between strains and displacement holds:

$$\boldsymbol{\epsilon} = \boldsymbol{D}\boldsymbol{u} \tag{18}$$

where the linear differential operator $\boldsymbol{D}$ is defined as follows:

$$\boldsymbol{D} = \begin{bmatrix}
0 & \frac{\partial}{\partial y} & 0 \\
\frac{\partial}{\partial x} & 0 & 0 \\
0 & 0 & \frac{\partial}{\partial z} \\
\frac{\partial}{\partial z} & 0 & \frac{\partial}{\partial x} \\
0 & \frac{\partial}{\partial z} & \frac{\partial}{\partial y} \\
\frac{\partial}{\partial y} & \frac{\partial}{\partial x} & 0
\end{bmatrix} \tag{19}$$

The stress components can be obtained then by the constitutive law:

$$\boldsymbol{\sigma} = \tilde{\boldsymbol{C}}\boldsymbol{\epsilon} \tag{20}$$

For the sake of brevity, the explicit form of the coefficients $\tilde{\boldsymbol{C}}_{ij}$ in the previous relation is omitted. More details can be found in [56, 57, 58].

5.2 PVD and fundamental nuclei

Adopting the FEM to discretize the structure along the y axis, the generalized displacements are interpolated by means of the 1D Lagrange shape functions N_i:

$$\boldsymbol{u} = F_\tau(x,z)N_i(y)\boldsymbol{q_{\tau i}} \tag{21}$$

The properties and the expressions of the shape functions are not reported in the present paper for the sake of brevity. A more detailed explanation of this procedure can be found in literature ([56, 57]). In the present work four-node (B4) 1D elements leading to cubic approximation along the y axis have been used. Employing the principle of virtual displacement, the internal strain energy L_{int} can be related to the work of the external and inertial loads, L_{ext} and L_{ine} respectively:

$$\delta L_{int} = \delta L_{ext} + \delta L_{ine} \tag{22}$$

Where δ stands for virtual variation. Considering a static problem:

$$\delta L_{int} = \int_V \left(\delta\boldsymbol{\epsilon}^T\boldsymbol{\sigma}\right) dV = -\delta L_{ext} \tag{23}$$

Considering the Eqs.(18),(17) and (21), the virtual variation of the strain energy can be written in a compact form:

$$\delta L_{int} = \delta\boldsymbol{q}_{\tau i}^T\mathbf{K}^{ij\tau s}\boldsymbol{q}_{sj} \tag{24}$$

The following algebraic system is obtained for static analysis :

$$\mathbf{Kq} = \mathbf{F} \tag{25}$$

The unknowns of the problem are the terms $\mathbf{q}$, that is the node displacements, whereas $\mathbf{K}$ indicates the assembled stiffness matrix and $\mathbf{F}$ stands for the equivalent nodal loadings. On the other hand, the work of the inertial loads can be written in terms of virtual variation:

$$\delta L_{ine} = \int_V \rho\ddot{\mathbf{u}}\delta\mathbf{u}^T\, dV \tag{26}$$

In the above equation ρ is the density of the material and $\ddot{u}$ is the acceleration vector. Taking into account the Eq. 3 and the finite element expansion in Eq. 21, the previous relation can be rearranged as reported below

$$\delta L_{ine} = -\delta \boldsymbol{q}_{\tau i}^T \int_l N_i N_j \, dy \int_\Omega \rho F_\tau F_s \, d\Omega \ddot{\mathbf{q}}_{sj} = -\delta \boldsymbol{q}_{\tau i}^T \mathbf{M}^{ij\tau s} \ddot{\mathbf{q}}_{sj} \tag{27}$$

where $\ddot{\mathbf{q}}_{sj}$ indicates the nodal acceleration vector and $\mathbf{M}^{ij\tau s}$ indicates the fundamental nucleus of the element mass matrix, whose components are:

$$\begin{gathered} \mathbf{M}_{xx}^{ij\tau s} = \mathbf{M}_{yy}^{ij\tau s} = \mathbf{M}_{zz}^{ij\tau s} = \textstyle\int_l N_i N_j \, dy \int \Omega \rho F_\tau F_s \, d\Omega \\ \mathbf{M}_{xy}^{ij\tau s} = \mathbf{M}_{xz}^{ij\tau s} = \mathbf{M}_{yx}^{ij\tau s} = \mathbf{M}_{zx}^{ij\tau s} = \mathbf{M}_{yz}^{ij\tau s} = \mathbf{M}_{zy}^{ij\tau s} = 0 \end{gathered} \tag{28}$$

Since no assumption has been made on the expansion order of the theory, several refined beam models can be developed without any formal changes in the fundamental nucleus components. The algebraic set of equations for the undamped dynamic problems is

$$\mathbf{M}\ddot{\mathbf{q}} + \mathbf{K}\mathbf{q} = 0 \tag{29}$$

Considering harmonic solutions, the natural frequencies ω_i can be evaluated in the homogeneous case solving the following eigenvalue problem:

$$(-\omega_i^2 \mathbf{M} + \mathbf{K})\mathbf{q}_i = 0 \tag{30}$$

where $\mathbf{q}_i$ is the *i-th* eigenvector.

Given the shape functions type and the class and the order of the cross-sectional functions F_τ, the 3x3 fundamental nucleus of the stiffness and the mass matrices, $K^{ij\tau s}$ and $M^{ij\tau s}$, can be computed. Subsequently, it can be automatically expanded to obtain the elemental stiffness and mass matrices, which are then assembled in the classical way of FEM. According to CUF, the expansion is made by employing four indexes: indexes τ and s are related to the functions F_τ and F_s, which define the beam model, whereas i and j are related to the shape functions N_i and N_j. The formal expression of the fundamental nucleus neither depend on the expansion order nor the choice of F_τ polynomials. Thus, TE, LE and CE models can be obtained by means of the same fundamental nucleus. Considering the properties mentioned above, the CUF enables to implement with a few coding statements any order of multiple class theories. A more detailed explanation of CUF fundamental nuclei and assembly procedure can be found in [59, 50].

6 Numerical Results

In the following section, the capabilities of CUF models with 2D Chebyshev polynomials of the second kind are investigated.

$w \times 10^{-3}(m)$				
Model	$5B4$	$10B4$	$30B4$	*Analytical*
EBBT	6.8503	6.8503	6.8503	6.8493
TBT	6.8508	6.8508	6.8508	6.8498
TE_1	6.8508	6.8508	6.8508	–
TE_3	6.7438	6.7912	6.8319	–
TE_5	6.7438	6.7912	6.8321	–
CE_1	4.4511	4.4511	4.4511	–
CE_3	6.7438	6.7912	6.8319	–
CE_5	6.7438	6.7912	6.8320	–

Table 1: w displacement values, isotropic square cantilever beam.

6.1 Cantilever beam with square, compact section

In order to perform a convergence study, a square section cantilever beam is considered. The beam cross-section has side dimension $a = b = 0.2$ m, with the length-to-thickness ratio equal to $L/h = 100$ (slender beam). The whole beam is made of aluminum alloy with Young's Modulus equal to 73 GPa, Poisson's ratio $\nu = 0.3$. The beam is clamped at $y = 0$ and a vertical point load $F_z = -25$ N is applied at the tip. The vertical displacement w has been computed with various meshes using Taylor and Chebyshev expansions, as shown in Table 1. Analytical results obtained with classical theories are provided for comparison. These results are obtained with the following formulas:

$$w_{EBBT} = \frac{F_z\, L^3}{3EI} \tag{31}$$

$$w_{TBT} = \frac{F_z\, L^3}{3EI} + \frac{F_z\, L}{AG} \tag{32}$$

where I is the moment of inertia with respect to the x axis and A indicates the area of the cross section. It is clear that classical theories provide a good approximation of the problem considered since all the theories considered yield similar results in the case of homogeneous isotropic solid-section beams subject to bending. However, it can be noticed that the CE_1 model, in which the Poisson locking phenomenon has occurred, has a deviation from the other results. For this reason, the CE_1 model isn not considered in the following analysis.

6.2 Rectangular thin walled box

Static and free vibration analysis of the thin walled box considered in [60, 61] are performed. The box has the following geometrical features: length $L = 3$ m, length-to-width ratio $L/b = 3.125$, cross-section height $h = 0.46$ m, thickness of the panels $t = 2 \times 10^{-3}$ m, spar caps area $A_s = 1.6 \times 10^{-3}\ m^2$. The structure is made of the same isotropic material as in the previous case, ($\rho = 2700\ kg/m^3$). A point load F_z having magnitude 1×10^4 N is applied in $[b, L, h/2]$, along the negative direction of the z axis. The structure is clamped at $y = 0$. The analysis are performed using Taylor, Chebyshev and Lagrange expansions on the section. The $L9$ mesh adopted for the first case is shown in Fig. 2a. Displacements and stresses resulting from static analysis

are shown in Table 2 and Fig. 3. The distribution of σ_{yz} along the z axis is evaluated in $[b, L/2]$ whereas the distribution of σ_{xy} along the x axis is evaluated in $[L/2, -h/2]$. Natural frequencies resulting from the free vibration analysis are reported in Table 3.

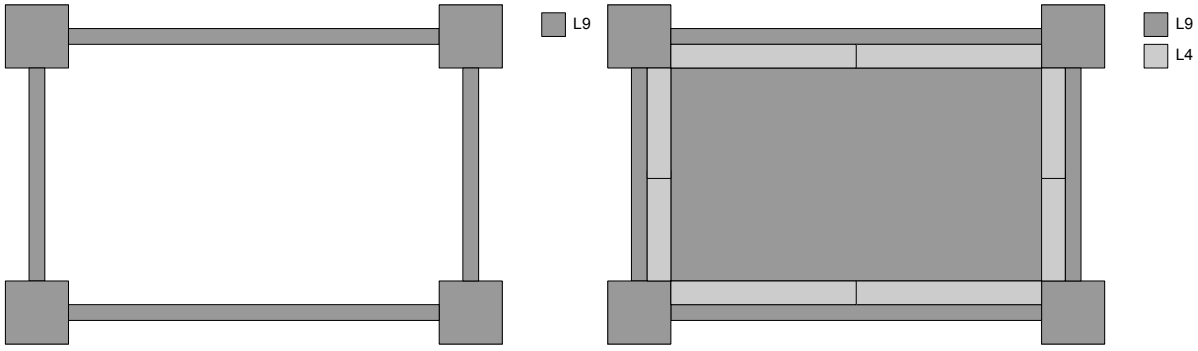

(a) Wing box LE mesh (b) Wing box with rib LE mesh

Figure 2: LE mesh of the two rectangular boxes.

Model	$w \times 10^{-3}$ (m)	$DOFs$
Classical beam theories		
EBBT	-2.147	93
TBT	-2.238	155
Taylor expansion		
TE_4	-3.038	1395
TE_6	-3.296	2604
TE_8	-5.421	4185
Chebyshev expansion		
CE_4	-3.009	1395
CE_6	-3.306	2604
CE_8	-5.748	4185
Lagrange expansion		
$8L9$	-6.144	5952

Table 2: w displacement values at the load application point, rectangular box without rib.

The results demonstrate the accuracy of the higher-order theories with respect to classical solutions. Column 3 of Table 2 reports the DOFs required for the different displacement models. Moreover, observing the graphs reported in Fig. 3(a) and (b) it can be noticed that classical approaches underestimate the stresses, whereas higher-order theories provide a more accurate approximation. Furthermore, it is clear that classical and lower order theories yield poor results in the case of free vibration analysis of thin-walled structures. Although these theories detect the bending modes, the shell-like modal shapes require higher-order and more refined theories to be evaluated.

A variant of the same structure, having a transversal stiffener at the free edge is then analyzed. The rib thickness is $r = t$. LE mesh adopted to model the rib is shown in Fig.2b. Static and free vibration analysis are carried out as previously, varying the theory expansion order. Results from static and free vibration analyses are shown in Table 4 and Table 5, respectively.

Although the addition of the rib, the limits of the EBBT and TBT models are undeniable in the detection of

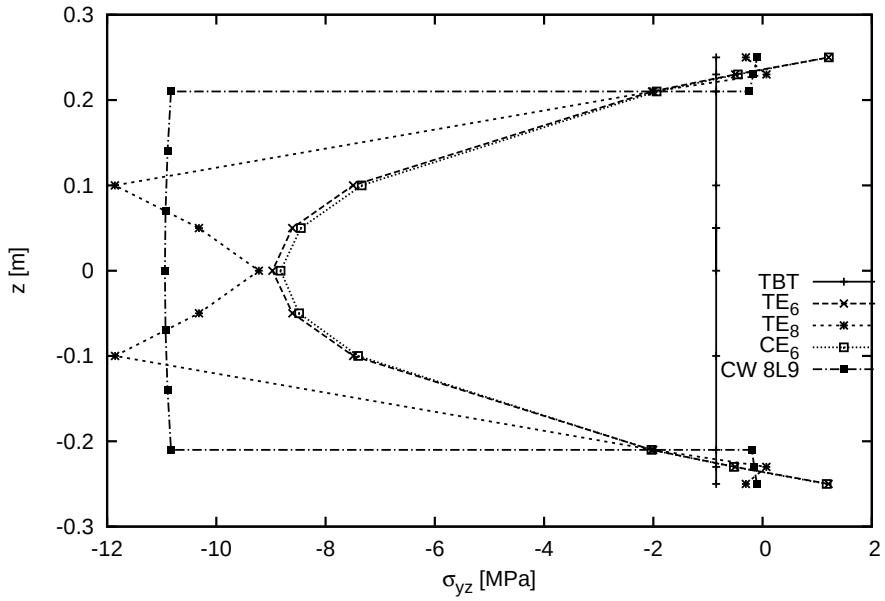

(a) σ_{yz} vs z at $x = b$, $y = \frac{L}{2}$

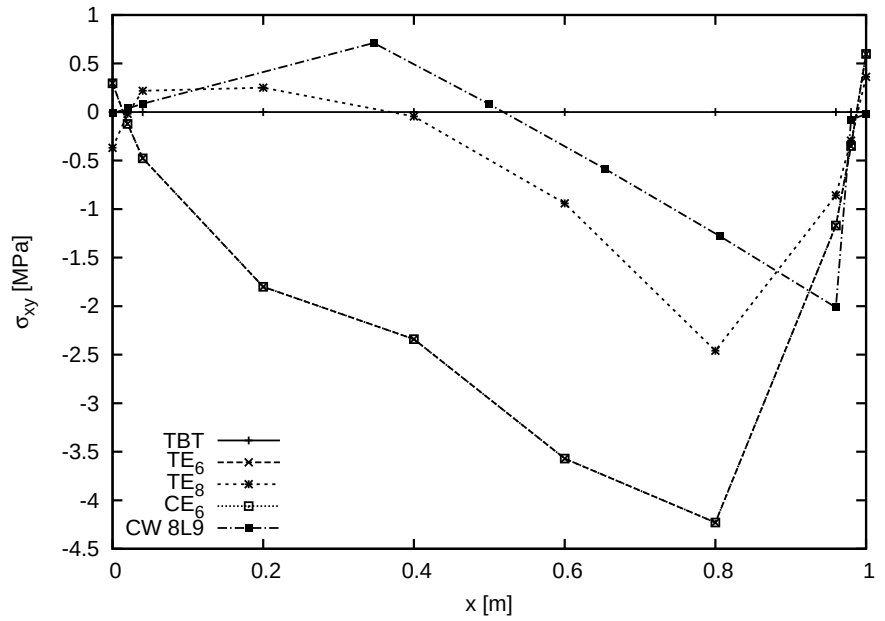

(b) σ_{xy} vs x at $z = \frac{-h}{2}$, $y = \frac{L}{2}$

Figure 3: Shear stress σ_{yz} vs the z-axis and σ_{xy} vs the x-axis, rectangular box without rib.

shell-like and non-classical effects. Also for this, the problem requires more refined and higher-order theories.

6.3 8-layer laminated beam

The cantilever 8-layer laminated beam investigated in [41] is considered. The geometry and the stacking sequence are shown in Fig.4. All layers have the same Young Modulus in the transverse direction $E_2 = 1$GPa, shear modulus $G = 0.5$ GPa, Poisson's ratio $\nu = 0.25$, whereas the layers labeled with 1 have longitudinal modulus $E_1 = 30$ GPa and the layers labeled with 2 have $E_1 = 5$ GPa. Ten four-node beam elements are

EBBT	TBT	TE_1	TE_3	TE_5	TE_7	CE_3	CE_5	$8L9$
DOFs								
93	155	279	930	1953	2376	930	1953	4860
I Differential bending								
–	–	–	–	$333.88^{(6)}$	$63.47^{(3)}$	–	$333.86^{(6)}$	$56.43^{(33)}$
I Bending along the $x-axis$								
$70.57^{(1)}$	$68.46^{(1)}$	$68.46^{(1)}$	$62.51^{(1)}$	$61.37^{(1)}$	$60.30^{(2)}$	$62.51^{(1)}$	$61.37^{(1)}$	$69.47^{(38)}$
I Bending along the $z-axis$								
$133.08^{(2)}$	$120.84^{(2)}$	$120.85^{(2)}$	$107.71^{(2)}$	$105.21^{(2)}$	$105.62^{(5)}$	$107.72^{(2)}$	$105.21^{(2)}$	$111.12^{(53)}$
I Torsional								
–	–	$269.29^{(3)}$	$224.50^{(3)}$	$135.81^{(3)}$	$166.54^{(7)}$	$224.50^{(3)}$	$135.81^{(3)}$	$153.49^{(62)}$
II Differential bending								
–	–	–	–	$563.20^{(12)}$	$244.99^{(13)}$	–	$563.20^{(12)}$	$247.33^{(81)}$
II Bending along the $x-axis$								
$413.43^{(3)}$	$352.05^{(3)}$	$352.05^{(4)}$	$249.46^{(4)}$	$241.78^{(5)}$	$203.45^{(10)}$	$249.46^{(4)}$	$241.78^{(5)}$	$266.92^{(84)}$
II Bending along the $z-axis$								
$678.26^{(5)}$	$473.86^{(5)}$	$473.87^{(6)}$	$369.42^{(5)}$	$352.77^{(7)}$	$336.31^{(22)}$	$369.42^{(5)}$	$352.77^{(7)}$	$364.08^{(95)}$
II Torsional Shell-like								
–	–	$807.88^{(7)}$	$608.32^{(8)}$	$392.66^{(8)}$	$430.06^{(31)}$	$608.32^{(8)}$	$392.62^{(8)}$	$456.16^{(101)}$
I Extensional								
$439.18^{(4)}$	$439.18^{(4)}$	$439.20^{(5)}$	$441.04^{(6)}$	$440.11^{(9)}$	$439.97^{(33)}$	$441.03^{(6)}$	$440.11^{(9)}$	$440.27^{(98)}$

Table 3: Natural frequencies of the box with no rib.

Model	$w \times 10^{-3}$ (m)	$DOFs$
Classical beam theories		
EBBT	-2.147	93
TBT	-2.238	155
Taylor expansion		
TE_4	-2.953	1395
TE_6	-3.047	2604
TE_8	-3.107	4185
Chebyshev expansion		
CE_4	-2.915	1395
CE_6	-3.001	2604
CE_8	-3.034	4185
Lagrange expansion		
$8L9$	-3.136	5952

Table 4: w displacement values at the load application point, rectangular box with rib.

EBBT	TBT	TE_1	TE_3	TE_5	CE_3	CE_5	$8L9$
DOFs							
102	170	306	1020	2142	1020	2142	4860
I Bending along the $x-axis$							
$67.41^{(1)}$	$65.47^{(1)}$	$65.47^{(1)}$	$59.99^{(1)}$	$58.92^{(1)}$	$59.99^{(1)}$	$58.92^{(1)}$	$64.68^{(33)}$
I Bending along the $z-axis$							
$127.40^{(2)}$	$116.02^{(2)}$	$116.02^{(2)}$	$103.74^{(2)}$	$101.41^{(2)}$	$103.74^{(2)}$	$101.41^{(2)}$	$107.15^{(49)}$
I Torsional							
–	–	$266.70^{(3)}$	$223.77^{(3)}$	$138.29^{(3)}$	$223.77^{(3)}$	$138.33^{(3)}$	$125.07^{(54)}$
I Differential bending							
–	–	–	–	$467.42^{(10)}$	–	$467.42^{(10)}$	$210.39^{(69)}$
II Bending along the $x-axis$							
$398.42^{(3)}$	$340.52^{(3)}$	$340.52^{(4)}$	$242.17^{(4)}$	$234.71^{(4)}$	$242.17^{(4)}$	$234.67^{(4)}$	$257.71^{(76)}$
II Bending along the $z-axis$							
$660.08^{(5)}$	$462.67^{(5)}$	$462.67^{(6)}$	$360.29^{(5)}$	$344.24^{(7)}$	$360.29^{(5)}$	$343.57^{(7)}$	$353.21^{(85)}$
II Torsional							
–	–	$799.90^{(8)}$	$641.42^{(8)}$	$366.59^{(8)}$	$641.42^{(8)}$	$366.70^{(8)}$	$369.19^{(88)}$
II Differential bending							
–	–	–	–	$737.18^{(16)}$	–	$741.90^{(17)}$	$509.66^{(98)}$
I Extensional							
$428.76^{(4)}$	$428.76^{(4)}$	$428.76^{(5)}$	$430.16^{(6)}$	$443.92^{(9)}$	$430.16^{(6)}$	$445.53^{(9)}$	$438.33^{(91)}$

Table 5: Natural frequencies of the wing box with a rib at the tip.

used to model the structure along y. A concentrated load $F_z = 0.2$ N is applied at the tip. Results in terms of maximum displacement and maximum longitudinal stress at mid-span are shown in Table 6 and compared with those available in literature. Moreover, σ_{yy} and σ_{yz} distributions along the z axis are reported in Fig.5. The results provided by TE expansions are in strong agreement with reference solutions available in [41] both in term of displacements and normal stresses. The classical TBT theory can be used as a good approximation for the evaluation of the axial stress σ_{yy}. However, refined beam theories are needed to evaluate the distribution of σ_{yz} along the z-axis. Moreover, the accordance between CE and TE models adopted for the analysis can

	$-w \times 10^{-2}$	$-\sigma_{yy}$	$DOFs$
Surana and Nguyen[8]	3.031	720	-
Davalos and Barbero[62]	3.029	700	-
Lin and Zhang[63]	3.060	750	-
Vo and Thai[64]	3.024	-	-
EBBT	2.629	730	279
TBT	2.988	730	279
TE_1	2.992	730	279
TE_2	2.985	730	558
TE_3	3.032	729	930
TE_5	3.042	730	1953
TE_8	3.046	730	4185
CE_2	2.992	730	558
CE_3	3.035	730	930
CE_5	3.040	730	1953
CE_8	3.046	730	4185

Table 6: w displacement and σ_{yy} values composite cantilever beam.

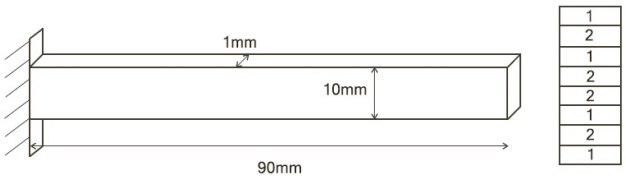

Figure 4: Eight-layer composite beam.

be pointed out.

6.4 Symmetric and antisymmetric cross-ply beam

Symmetric (0/90/0) and antisymmetric (0/90) cross-ply laminated beams whose static analysis has been carried out in [41] are then considered. All the laminae have the same thickness and made of the orthotropic material having the following properties:

$$\frac{E_L}{E_T} = 25 \qquad \frac{G_{LT}}{G_{TT}} = 2.5$$
$$G_{TT} = 0.2E_T \quad \nu_{LT} = \nu_{TT} = 0.25$$

where L indicates the fiber direction whereas T the transverse direction. The Clamped-Free (CF) boundary conditions are imposed whereas a uniform load is distributed on the lower face. Static analyses are performed varying length-to-thickness ratio L/h = 5, 10, 20. Results are reported in Table 7 and 8 for the symmetric cross-ply and the antisymmetric cross-ply cases, respectively. The results have been normalized using the formula adopted in [41]:

$$\bar{w} = 100 \cdot \frac{b \cdot h^3}{q_o L^4} \cdot w \tag{33}$$

It is clear that the static behavior of laminated beams cannot be accurately described by means of the classical theories (EBBT and TBT), especially when the aspect ratio decreases. The use of Taylor-like Expansion and

	$\bar{w}$		
L/h	5	10	20
	Khdeir et al.[4]		
CBT	2.198	2.198	2.198
FOBT	6.698	3.323	–
HOBT	6.824	3.455	–
	Vo and Thai [64]		
CBT	2.203	2.203	2.203
FOBT	6.703	3.328	2.485
HOBT	6.830	3.461	2.530
SSBT	6.842	3.478	2.536
EBBT	2.205	2.203	2.203
TBT	5.953	3.139	2.437
TE_1	5.953	3.139	2.437
TE_2	5.946	3.135	2.433
TE_3	7.154	3.511	2.537
TE_6	7.289	3.574	2.56
CE_2	5.947	3.135	2.433
CE_3	7.155	3.511	2.537
CE_6	7.290	3.574	2.56
CBT:	Classical Beam Theory		
FOBT:	First Order Beam Theory		
HOBT:	Higher-Order Beam Theory		
SSBT:	Sinusoidal Shear Beam Theory		

Table 7: $\bar{w}$ mid-span displacement of a symmetric cross-ply cantilever beam subject to uniform load.

	$\bar{w}$		
L/h	5	10	20
	Khdeir et al.[4]		
CBT	11.293	11.293	11.293
FOBT	16.436	12.579	–
HOBT	15.279	12.343	–
	Vo and Thai [64]		
CBT	11.319	11.319	11.319
FOBT	16.461	12.604	11.640
HOBT	15.305	12.369	11.588
SSBT	15.173	12.340	11.582
EBBT	11.31	11.31	11.31
TBT	15.606	12.383	9.263
TE_1	13.087	11.754	11.421
TE_2	15.641	12.375	11.552
TE_5	16.202	12.539	11.603
TE_6	16.205	12.540	11.603
CE_2	15.642	12.375	11.552
CE_5	16.202	12.540	11.603
CE_6	16.206	12.540	11603

Table 8: $\bar{w}$ mid-span displacement of an antisymmetric cross-ply cantilever beam.

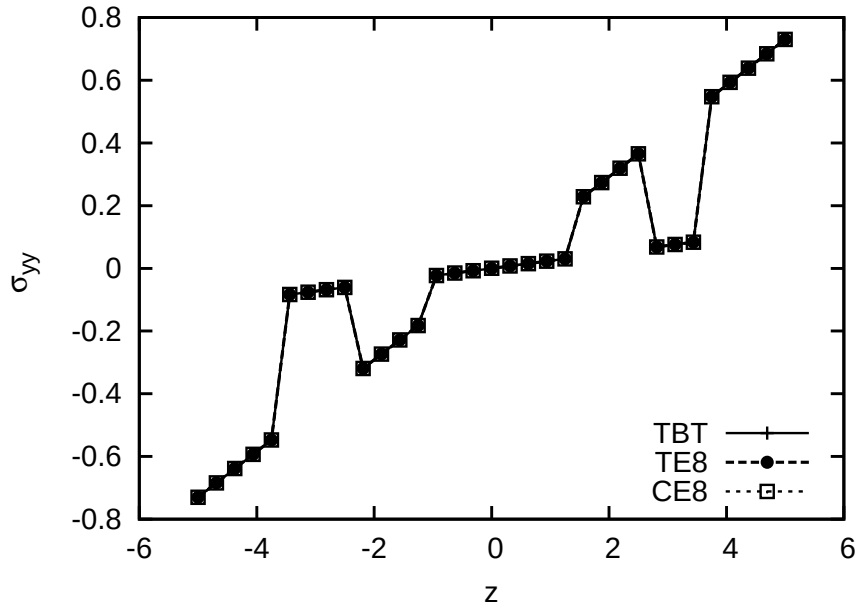

(a) σ_{yy} vs z at mid-span

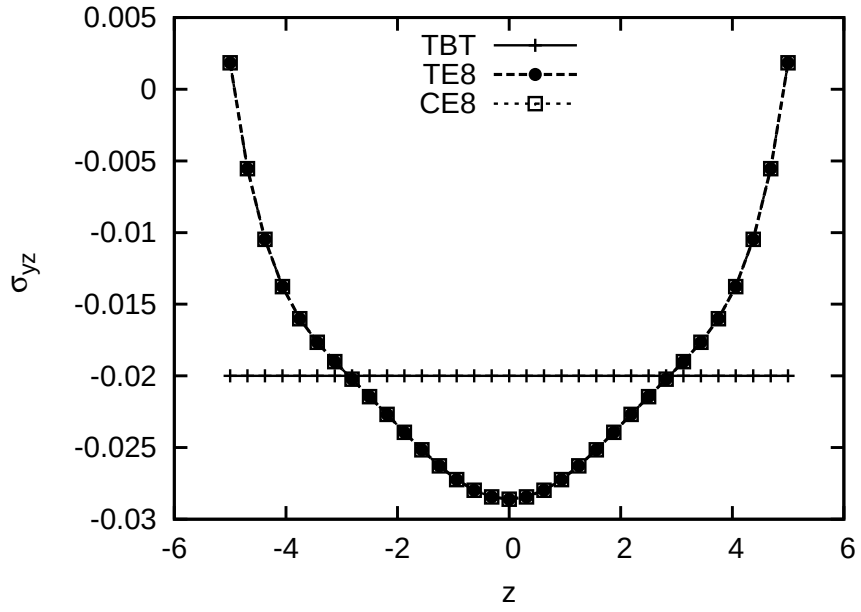

(b) σ_{yz} vs z at mid-span

Figure 5: Axial stress σ_{yy} and shear stress σ_{yz} vs. the z-axis, eight-layer composite beam.

Chebyshev Expansion polynomials introduces significant improvements in the model. The results obtained by means of higher-order CE and TE models show good accordance with the reference solutions. It should be noted that the reference solutions found in literature include a shear correction factor of $\frac{5}{6}$, whereas the adopted TBT theory does not account it.

Mode	I^b	II^b	III^b	IV^b	V^b	VI^b	VII^b	$VIII^c$	IX^c
Exper.[65]	–	–	185.50	280.30	399.40	535.20	680.70	–	–
[66]	34.597	93.100	177.16	282.78	406.33	544.33	693.79	–	–
DSM [67]	34.342	91.385	171.69	270.36	383.27	506.88	638.39	–	–
FEM 3D [58]	34.817	93.676	178.20	284.37	408.44	546.93	696.77	298.97	598.88
EBBT	35.433	97.663	191.43	316.36	472.46	659.64	877.86	–	–
TBT	35.416	97.558	191.07	315.48	470.60	656.18	871.94	–	–
TE_1	35.416	97.558	191.07	315.48	470.60	656.18	871.94	1137.8	2275.6
TE_2	35.540	97.899	191.75	316.61	472.31	658.61	875.24	865.47	1731.2
TE_4	35.068	95.137	182.79	294.95	428.66	580.89	748.74	362.57	725.69
TE_7	35.037	94.497	180.31	288.63	416.12	559.18	715.42	336.01	672.52
CE_2	35.540	97.899	191.75	316.61	472.31	658.61	875.25	865.47	1731.2
CE_4	35.068	95.137	182.79	294.96	428.66	580.88	748.74	362.57	725.69
CE_7	35.037	94.498	180.31	288.63	416.12	559.18	715.42	336.01	672.52

[b]:bending mode in z-direction.
[c]:torsional mode.

Table 9: Natural frequencies (Hz) of the rectangular clamped clamped sandwich beam.

6.5 Sandwich beam

Two sandwich beams whose free vibration analysis has been performed in [58] are considered. The structures consist of two face sheets (f) bonded to a core (c) whose properties are:

$$E_f = 68.9GPa \quad E_c = 179.014MPa \quad G_f = 26.5GPa$$
$$G_c = 68.9MPa \quad \rho_f = 2687.3kg/m^3 \quad \rho_c = 119.69kg/m^3$$

The first case is a clamped-clamped sandwich beam having rectangular cross-section, whose geometrical features are the following: $h_f = 0.40624$ mm, $h_c = 6.3475$ mm, $b = 25.4$ mm, $L = 1.2187$ m. Natural frequencies are reported in Table 9.

The first seven flexural modes on the yz-plane and the first two torsional ones are evaluated. It should be noted that the expansions TE_7 and CE_7 provide the closest result with respect to the reference solution reported in [58] for the two latter modes.

In the second case, a square cross-section beam having the previous boundary conditions is considered. Length-to-thickness $\frac{L}{h}$ ratio is set to 5 whereas core-to-face ratio $\frac{h_c}{h_f}$ is assumed to be 8. Dimensionless frequencies obtained using the 34 have been reported in Table 10.

$$\bar{\omega} = \frac{L^2}{b} \cdot \sqrt{\frac{\rho_f}{G_f}} \cdot \omega \tag{34}$$

It can be highlighted that the dynamic behavior of the sandwich deep beams can be accurately described only by means of refined kinematic models. Observing the modal shapes of the structure, it can be noted that the VII and VIII modal shape ((6b) and (6c)), involve important deformations of the core. Thus, these modes cannot be described through classical theories. Moreover, the VI frequency is characterized by an antisymmetric modal shape with respect to the yz-plane (see Fig. (6a)) that requires a refined theory to be

Mode	I^b	II^b	III^c	IV^b	V^a	VI^*	VII^*	$VIII^*$	DOFs
FEM $3D$ [58]	2.0308	4.3874	6.6198	7.3156	7.7618	10.461	10.603	10.673	68277
EBBT	14.374	35.788	–	61.874	9.450	–	–	–	279
FSDT	10.368	22.117	–	35.738	7.980	–	–	–	279
TE_1	10.368	22.117	15.117	35.738	7.980	30.232	87.823	–	279
TE_3	3.511	7.249	13.774	11.524	7.926	31.661	21.485	–	930
TE_6	2.284	4.879	7.056	8.034	7.821	11.853	12.332	12.269	2604
TE_7	2.281	4.872	7.011	8.024	7.819	11.840	11.915	12.270	3348
CE_3	3.511	7.249	13.774	11.524	7.926	31.661	21.485	–	930
CE_6	2.284	4.879	7.056	8.034	7.821	11.853	12.332	12.269	2604
CE_7	2.281	4.872	7.011	8.024	7.819	11.840	11.915	12.270	3348

$*$:modes in Fig. 6
^{a}:bending mode in x-direction.
^{b}:bending mode in z-direction.
^{c}:torsional mode.

Table 10: Dimensionless frequencies of the square clamped-clamped sandwich beam, L/h = 5.

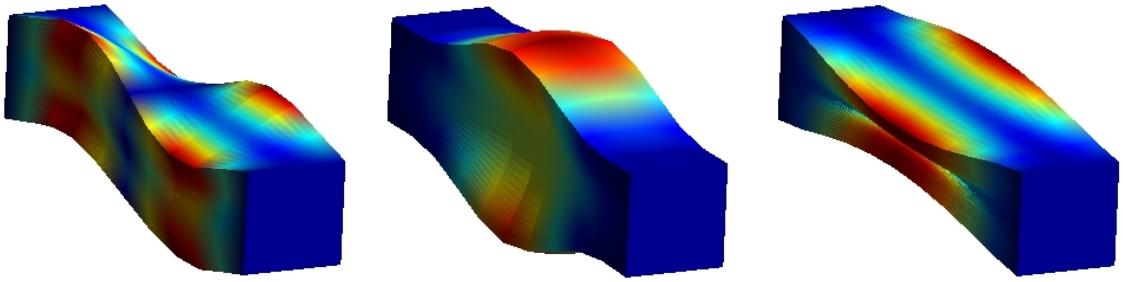

(a) Mode VI (b) Mode VII (c) Mode VIII

Figure 6: Modal shapes of the sandwich square section beam, CE_7.

detected.

6.6 4-layer composite box beam

A thin-walled composite box beam is then considered. The material properties are:

$$E_L = 144GPa \quad E_T = 9.65GPa \quad G_{LT} = 4.14GPa$$
$$G_{TT} = 3.45GPa \quad \nu_{LT} = \nu_{TT} = 0.3 \quad \rho = 1389kg/m^3$$

The lenght-to-thickness ratio $\frac{L}{h}$ is equal to 6.667 whereas the $\frac{h}{b}$ is 2 and $\frac{b}{t_e}$ is equal to 10. As result of free vibration analysis, the first 8 frequencies for three different lamination cases (0/0/0/0),(0/90/90/0),(45/-45/-45/45) are reported in Table 11.

Although the complexity of the structure, a good level of accuracy is obtained by means of the variable kinematic models. The shell-like modes of the box with the first lamination scheme are shown in Fig. 7. The V frequency is characterized by an anti-symmetric modal shape with respect to the yz-plane, whereas the IX mode presents the anti-symmetric modal shape in the yx-plane. The symmetric deformations of the walls with one, two and three half-waves along the longitudinal axis are shown in figures 7(b),7(c),7(d) respectively.

Mode	I	II	III	IV	V	VI	VII	$VIII$	IX	X
					0/0/0/0					
Shell[58]	35.447^{a}	58.533^{b}	$76.011^{c/d}$	114.23^{d}	130.12^{d}	143.15^{d}	148.53^{d}	163.65^{d}	165.24^{d}	$170.34^{a/d}$
TE_2	43.464	64.526	98.508	196.87	–	–	–	–	–	–
TE_4	38.345	60.171	89.810	144.93	851.27	1211.7	1215.8	1234.5	–	292.79
TE_5	37.402	59.461	89.221	139.15	420.22	371.27	436.60	392.62	257.92	636.23
CE_2	43.464	64.526	98.508	196.87	–	–	–	–	–	–
CE_4	38.345	60.171	89.810	144.93	851.27	1211.7	1215.8	1234.5	–	292.79
CE_5	37.402	59.461	89.222	139.13	420.30	371.16	436.95	–	392.63	636.21
					0/90/90/0					
Shell [58]	29.129^{a}	48.813^{b}	$81.335^{c/d}$	112.37^{a}	179.21^{d}	182.70^{b}	197.83^{d}	$205.38^{a/d}$	232.92^{d}	235.97^{d}
TE_2	33.087	51.562	96.588	165.08	–	–	–	–	–	–
TE_4	30.677	49.286	88.938	129.57	909.06	191.75	890.10	273.56		
TE_5	30.170	48.954	88.506	124.86	484.71	489.46	503.84	533.93	257.79	261.33
CE_2	33.087	51.562	96.589	165.08	–	–	–	–	–	–
CE_4	30.677	49.286	88.938	129.57	909.06	191.75	890.10	273.56		
CE_5	30.170	48.958	88.506	124.87	484.68	489.67	504.08	534.23	257.80	261.29
					$45/-45/-45/45$					
Shell[58]	15.803^{a}	26.041^{b}	96.012^{a}	153.84^{b}	$168.38^{c/d}$	197.92^{d}	209.19^{e}	$237.73^{a/d}$	267.17^{d}	272.02^{d}
TE_2	17.628	29.576	108.26	–	–	–	–	–	–	–
TE_4	16.580	27.842	102.24	164.21	249.34	633.33	220.48	280.23	758.83	–
TE_5	16.425	26.822	101.402	164.05	239.68	524.94	553.42	605.20	423.35	214.38
CE_2	17.628	29.576	108.26	–	–	–	–	–	–	–
CE_4	16.580	27.843	102.24	164.20	249.34	633.33	220.48	280.22	758.82	–
CE_5	16.424	27.822	101.40	164.05	239.69	524.49	553.81	606.73	423.59	214.38

[a]:bending mode in x-direction.
[b]:bending mode in z-direction.
[c]:torsional mode.
[d]:shell-like mode.
[e]:axial mode.

Table 11: First ten frequencies (Hz) of the thin-walled composite cantilever beam.

It is clear that the order of appearance of each mode and its frequency depends on the stacking sequences (e.g. the appearance of torsional modes). The enrichment of the displacement field strongly improves the solution, although the convergence to the reference data depends on the modal shape considered.

6.7 6-layer composite box beam

The model investigated has been considered in previous works within the framework of analytical [68], FEM [69] and experimental [70] approach, whereas Carrera Unified Formulation was used in [71]. The structure consists in a 6-layer laminated box beam with hollow rectangular cross-section, whose dimensions are: length $L = 844.55$ mm, height $h = 13.6$ mm, width $b = 24.2$ mm and thickness $t = 0.762$ mm. Each layer has the same thickness. The whole structure is made of the same orthotropic material, having

$$E_1 = 141.96GPa \quad E_2 = E_3 = 9.79GPa \quad \nu_{12} = \nu_{13} = 0.42$$
$$\nu_{23} = 0.5 \qquad G_{12} = G_{13} = 6.0GPa \quad G_{23} = 4.83GPa$$
$$\rho = 1445.0 \frac{kg}{m^3}$$

Different stacking sequences and ply angles have been considered, according to circumferentially asymmetric stiffness (CAS) and circumferentially uniform stiffness (CUS) schemes reported in Table 12. The natural

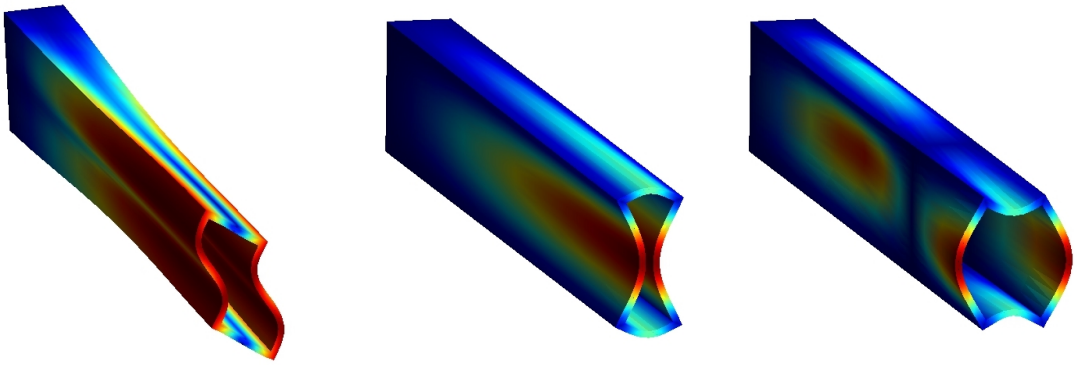

(a) Mode V (b) Mode VI (c) Mode VII

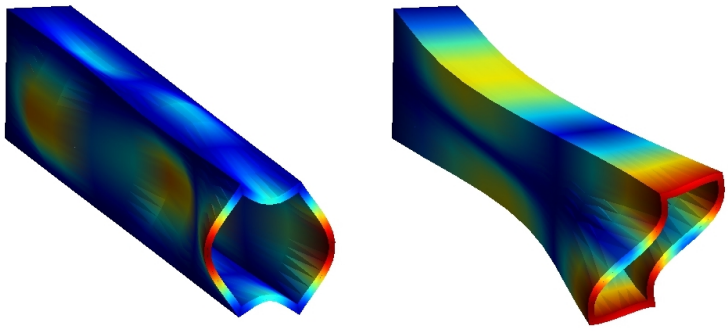

(d) Mode VIII (e) Mode IX

Figure 7: Modal shapes of the 0/0/0/0 laminated thin-walled box beam, CE_7.

	Flanges		Webs	
Layup	Top	Bottom	Left	Right
$CAS2$	$[30]_6$	$[30]_6$	$[30/-30]_3$	$[30/-30]_3$
$CAS3$	$[45]_6$	$[45]_6$	$[45/-45]_3$	$[45/-45]_3$
$CUS1$	$[15]_6$	$[-15]_6$	$[15]_6$	$[-15]_6$
$CUS2$	$[0/30]_3$	$[0/-30]_3$	$[0/30]_3$	$[0/-30]_3$
$CUS3$	$[0/45]_3$	$[0/-45]_3$	$[0/45]_3$	$[0/-45]_3$

Table 12: Various stacking sequences of the 6-layer box beam.

frequencies are listed in Table 13

The results reveal the correspondence of Chebyshev models and Taylor models. Furthermore, the analytical and experimental solutions are well approximated by higher order and Lagrange theories, whereas the limits of classical TBT and lower order theories are demonstrated.

		CUF LE	CUF TE			CUF CE			
Layup	Mode	$24L9$	TBT	TE3	TE7	CE3	CE7	Exp.	Analytical
$CAS2$	1^a	20.06	20.96	21.39	20.18	21.39	20.18	20.96	19.92
	2^b	38.21	41.75	40.51	38.47	40.51	38.47	38.06	–
	3^a	125.44	130.99	133.75	126.08	133.75	126.08	128.36	124.73
$CAS3$	1^a	14.75	15.01	15.25	14.77	15.25	14.77	16.67	14.69
	2^b	25.41	26.38	26.17	25.44	26.17	25.44	29.48	–
	3^a	92.35	93.87	95.43	92.38	95.43	92.38	96.15	92.02
$CUS1$	1^a	29.51	32.36	30.29	28.86	30.29	28.86	28.66	28.67
$CUS2$	1^a	34.69	35.09	35.00	34.61	35.00	34.61	30.66	34.23
$CUS3$	1^a	33.03	33.11	33.13	33.00	33.13	33.00	30.00	32.75

^{a} Flexural on plane yz; ^{b} Flexural on plane xz.

Table 13: Natural frequencies (Hz) for different stacking sequences of the six-layer laminated box beam.

7 Conclusions

In the present work, static and free vibration analyses of thin-walled, laminated, sandwich and composite beams have been carried out. The analyses were performed by means of the novel refined beam model based on the Chebyshev Expansion of the second kind within the framework of Carrera Unified Formulation. The results were compared to those published in the literature obtained through TE and LE CUF models, commercial MSC Nastran code, experimental and analytical data. Refined models have proved to be capable of overcoming the well-known limits of classical beam theories. The detection of torsion, coupling, in-plane deformation and shell-like behavior is enabled. CE CUF models allow to perform structure analyses with a high level of accuracy, preserving the low computational cost typical of the 1D approach. Moreover, the correspondence between existing TE and CE models has been demonstrated. An axiomatic asymptotic analysis similar to that performed in [34] might offer interesting information about the contribution of each higher-order term in the CE model.

References

[1] L. Euler. *De curvis elasticis*. Bousquet, Geneva, 1744.

[2] S.P. Timoshenko. On the corrections for shear of the differential equation for transverse vibration of prismatic bars. *Philosophical Magazine*, 41:744–746, 1922. doi: 10.1080/14786442108636264.

[3] S.P. Timoshenko. On the transverse vibrations of bars of uniform cross section. *Philosophical Magazine*, 41:122–131, 1922. doi: 10.1080/14786442208633855.

[4] A.A. Khdeir and J.N. Redd. Buckling of cross-ply laminated beams with arbitrary boundary conditions. *Composite Structures*, 37(1):1–3, 1997. doi: 10.1016/S0263-8223(97)00048-2.

[5] A.A. Khdeir and J.N. Redd. An exact solution for the bending of thin and thick cross-ply laminated beams. *Composite Structures*, 37(2):195–203, 1997. doi: 10.1016/S0263-8223(97)80012-8.

[6] A.A. Khdeir. Dynamic response of antisymmetric cross-ply laminated composite beams with arbitrary boundary conditions. *International Journal of Engineering Science*, 34(1):9–19, 1996. doi: 10.1016/0020-7225(95)00080-1.

[7] J.N. Reddy. A simple higher order theory for laminated composites. *Journal of Applied Mechanics*, 51:745–752, 1984. doi: 10.1115/1.3167719.

[8] K.S Surana and S.H Nguyen. Two-dimensional curved beam element with higher-order hierarchical transverse approximation for laminated composites. *Computers and Structures*, 36(3):499–511, 1990. doi: 10.1016/0045-7949(90)90284-9.

[9] M. Kameswara Rao, Y.M. Desai, and M.R. Chitnis. Free vibrations of laminated beams using mixed theory. *Composite Structures*, 52(2):149–160, 2001. doi: 10.1016/S0263-8223(00)00162-8.

[10] W. Yu and D. H. Hodges. Generalized Timoshenko theory of the variational asymptotic beam sectional analysis. *Journal of the American Helicopter Society*, 50(1):46–55, 2005. doi: 10.4050/1.3092842.

[11] L. Dufort, S. Drapier, and M. Grédiac. Closed-form solution for the cross-section warping in short beams under three-point bending. *Composite Structures*, 52(2):233–246, 2001. doi: 10.1016/S0263-8223(00)00171-9.

[12] P. Subramanian. Dynamic analysis of laminated composite beams using higher order theories and finite elements. *Composite Structures*, 73(3):342–353, 2006. doi: 10.1016/j.compstruct.2005.02.002.

[13] M. Karama, K.S. Afaq, and S. Mistou. Mechanical behaviour of laminated composite beams by the new multi-layered laminated composite structures model with transverse shear stress continuity. *International Journal of Solids and Structures*, 40:1525–1546, 2003. doi: 10.1016/S0020-7683(02)00647-9.

[14] M. S. Qatu. Theories and analyses of thin and moderately thick laminated composite curved beams. *International Journal of Solids and Structures*, 30(20):2743–2756, 1993. doi: 10.1016/0020-7683(93)90152-W.

[15] M. Hajianmaleki and M. S. Qatu. A rigorous beam model for static and vibration analysis of generally laminated composite thick beams and shafts. *International Journal of Vehicle Noise and Vibration*, 8(2):166–184, 2012. doi: 10.1504/IJVNV.2012.046464.

[16] M. Eisenberger, H. Abramovich, and O. Shulepov. Dynamic stiffness analysis of laminated beams using a first order shear deformation theory. *Composite Structures*, 31(4):265–271, 1995. doi: 10.1016/0263-8223(95)00091-7.

[17] L. Jun and H. Hongxing. Dynamic stiffness analysis of laminated composite beams using trigonometric shear deformation theory. *Composite Structures*, 89(3):433–442, 2009. doi: 10.1016/j.compstruct.2008.09.002.

[18] V.H. Cortínez and M.T. Piovan. Vibration and buckling of composite thin-walled beams with shear deformability. *Journal of Sound and Vibration*, 258(4):701–723, 2002. doi: 10.1006/jsvi.2002.5146.

[19] M. Mitra, S. Gopalakrishnan, and M. S. Bhat. A new super convergent thin walled composite beam element for analysis of box beam structures. *International journal of solids and structures*, 41(5):1491–1518, 2004. doi: 10.1016/j.ijsolstr.2003.10.024.

[20] P. Vidal, L. Gallimard, and O. Polit. Composite beam finite element based on the proper generalized decomposition. *Computers and Structures*, 102-103(0):76–86, 2012. doi: 10.1016/j.compstruc.2012.03.008.

[21] J.L. Mantari, A.S. Oktem, and C. Guedes Soares. A new higher order shear deformation theory for sandwich and composite laminated plates. *Composites Part B: Engineering*, 43(3):1489–1499, 2012. doi: 10.1016/j.compositesb.2011.07.017.

[22] N. Grover, D.K. Maiti, and B.N. Singh. A new inverse hyperbolic shear deformation theory for static and buckling analysis of laminated composite and sandwich plates. *Composite Structures*, 95(0):667–675, 2013. doi: 10.1016/j.compstruct.2012.08.012.

[23] R.P. Shimpi and Y.M. Ghugal. A new layerwise trigonometric shear deformation theory for two-layered cross-ply beams. *Composites Science and Technology*, 61(9):1271–1283, 2001. doi: 10.1016/S0266-3538(01)00024-0.

[24] M. Tahani. Analysis of laminated composite beams using layerwise displacement theories. *Composite Structures*, 79(4):535–547, 2007. doi: 10.1016/j.compstruct.2006.02.019.

[25] H. Murakami. Laminated composite theory with improved in-plane responses. *Journal of Applied Mechanics*, 53:661–666, 1986. doi: 10.1115/1.3171828.

[26] P. Vidal and O. Polit. Assessment of the refined sinus model for the non-linear analysis of composite beams. *Composite Structures*, 87(4):370–381, 2009. doi: 10.1016/j.compstruct.2008.02.007.

[27] P. Vidal and O. Polit. A sine finite element using a zig-zag function for the analysis of laminated composite beams. *Composites Part B: Engineering*, 42(6):1671–1682, 2011. doi: 10.1016/j.compositesb.2011.03.012.

[28] E. Onate, A. Eijo, and S. Oller. Simple and accurate two-noded beam element for composite laminated beams using a refined zigzag theory. *Computer Methods in Applied Mechanics and Engineering*, 213-216(0):362–382, 2012. doi: 10.1016/j.cma.2011.11.023.

[29] R.K. Kapania and S. Raciti. Recent advanced analysis of laminated beams and plates. part i: shear effects and buckling. *AIAA Journal*, 27:923–934, 1989. doi: 10.2514/3.10202.

[30] Y. M. Ghugal and R. P. Shimpi. A review of refined shear deformation theories of isotropic and anisotropic laminated plates. *Journal of Reinforced Plastics and Composites*, 21(9):775–813, 2002. doi: 10.1177/073168402128988481.

[31] E. Carrera. Theories and finite elements for multilayered, anisotropic, composite plates and shells. *Archives of Computational Methods in Engineering*, 9(2):87–140, 2002. doi: 10.1007/BF02736649.

[32] E. Carrera. Theories and finite elements for multilayered plates and shells: a unified compact formulation with numerical assessment and benchmarking. *Archives of Computational Methods in Engineering*, 10(3):216–296, 2003. doi: 10.1007/BF02736224.

[33] E. Carrera and G. Giunta. Refined beam theories based on a unified formulation. *International Journal of Applied Mechanics*, 2(1):117–143, 2010. doi: 10.1142/S1758825110000500.

[34] E. Carrera and M. Petrolo. On the effectiveness of higher-order terms in refined beam theories. *Journal of Applied Mechanics*, 78, 2011. doi: 10.1115/1.4002207.

[35] E. Carrera, G. Giunta, and M. Petrolo. *A Modern and Compact Way to Formulate Classical and Advanced Beam Theories*, chapter 4, pages 75–112. Saxe-Coburg Publications, Stirlingshire, UK, 2010. doi: 10.4203/csets.25.4.

[36] E. Carrera, M. Petrolo, and A. Varello. Advanced beam formulations for free vibration analysis of conventional and joined wings. *Journal of Aerospace Engineering*, 25(2), 2012. doi: 10.1061/(ASCE)AS.1943-5525.0000130.

[37] M. Petrolo, E. Zappino, and E. Carrera. Unified higher-order formulation for the free vibration analysis of one-dimensional structures with compact and bridge-like cross-sections. *Thin Walled Structures*, 56, 2012. doi: 10.1016/j.tws.2012.03.011.

[38] S.M. Ibrahim, E. Carrera, M. Petrolo, and E. Zappino. Buckling of composite thin walled beams by refined theory. *Composite Structures*, 94(2):563–570, 2012. doi: 10.1016/j.compstruct.2011.08.020.

[39] S.M. Ibrahim, E. Carrera, M. Petrolo, and E. Zappino. Buckling of thin walled beams by refined theory. *Journal of Zhejiang University. Science A*, 2012. doi: 10.1631/jzus.A1100331.

[40] E. Carrera and M. Petrolo. Refined beam elements with only displacement variables and plate/shell capabilities. *Meccanica*, 47(3):537–556, 2012. doi: 10.1007/s11012-011-9466-5.

[41] E. Carrera, M. Filippi, and E. Zappino. Laminated beam analysis by polynomial, trigonometric, exponential and zig-zag theories. *European Journal of Mechanics - A/Solids*, 41(0):58 – 69, 2013. doi: 10.1016/j.euromechsol.2013.02.006.

[42] E. Carrera, M. Maiaru, and M. Petrolo. Component-wise analysis of laminated anisotropic composites. *International Journal of Solids and Structures*, 49:1839–1851, 2012. doi: 10.1016/j.ijsolstr.2012.03.025.

[43] D. Zhou, F.T.K. Au, Y.K. Cheung, and S.H. Lo. Three-dimensional vibration analysis of circular and annular plates via the Chebyshev-Ritz method. *International Journal of Solids and Structures*, 40(12):3089 – 3105, 2003. doi: 10.1016/S0020-7683(03)00114-8.

[44] D. Zhou, Y.K Cheung, F.T.K Au, and S.H Lo. Three-dimensional vibration analysis of thick rectangular plates using Chebyshev polynomial and Ritz method. *International Journal of Solids and Structures*, 39(26):6339 – 6353, 2002. doi: 10.1016/S0020-7683(02)00460-2.

[45] S.C. Sinha and E.A. Butcher. Solution and stability of a set of p th order linear differential equations with periodic coefficients via Chebyshev polynomials. *Mathematical Problems in Engineering*, 2(2):165–190, 1996. doi: 10.1155/S1024123X96000294.

[46] S.C. Sinha and E.A. Butcher. Symbolic computation of fundamental solution matrices for linear time-periodic dynamical systems. *Journal of Sound and Vibration*, 206(1):61 – 85, 1997. doi: 10.1006/jsvi.1997.1079.

[47] Y. Nath and K. Sandeep. Chebyshev series solution to non-linear boundary value problems in rectangular domain. *Computer Methods in Applied Mechanics and Engineering*, 125(14):41 – 52, 1995. doi: 10.1016/0045-7825(95)00801-7.

[48] M.Sari and E.A. Butcher. Natural frequencies and critical loads of beams and columns with damaged boundaries using Chebyshev polynomials. *International Journal of Engineering Science*, 48(10):862 – 873, 2010. doi: 10.1016/j.ijengsci.2010.05.008.

[49] P. Ruta. The application of Chebyshev polynomials to the solution of the nonprismatic timoshenko beam vibration problem. *Journal of Sound and Vibration*, 296(1–2):243–263, 2006. doi: 10.1016/j.jsv.2006.02.011.

[50] E. Carrera, M. Petrolo, and P. Nali. Unified formulation applied to free vibrations finite element analysis of beams with arbitrary section. *Shock and Vibration*, 18(3):485–502, 2011. doi: 10.3233/SAV-2010-0528.

[51] A. Pagani, M. Boscolo, J. R. Banerjee, and E. Carrera. Exact dynamic stiffness elements based on one-dimensional higher-order theories for free vibration analysis of solid and thin-walled structures. *Journal of Sound and Vibration*, 332(23):6104–6127, 2013. doi: 10.1016/j.jsv.2013.06.023.

[52] E. Carrera, G. Giunta, and M. Petrolo. *Beam Structures Classical and Advanced Theories*. John Wiley & Sons, Ltd, The Atrium, Southern Gate, Chichester, West Sussex, PO19 8SQ, United Kingdom, 2011.

[53] E. Carrera, M. Cinefra, M. Petrolo, and E. Zappino. *Finite Element Analysis of Structures through Unified Formulation*. John Wiley & Sons Ltd, 2014.

[54] K. Dunn and R. Lidl. Generalizations of the classical chebyshev polynomials to polynomials in two variables. *Czechoslovak Mathematical Journal*, 32:516–528, 1982.

[55] T.H. Koornwinder. Orthogonal polynomials in two variables which are eigenfunction of two algebraically independent partial differential operators, III. *Indagationes Mathematicae*, 77(4):357–381, 1974. doi: 10.1016/1385-7258(74)90026-2.

[56] S. W. Tsai. *Composites Design*. Dayton, Think Composites, 4th edition, 1988.

[57] J. N. Reddy. *Mechanics of laminated composite plates and shells. Theory and Analysis*. CRC Press, 2nd edition, 2004.

[58] E. Carrera, M. Filippi, and E. Zappino. Free vibration analysis of laminated beam by polynomial, trigonometric, exponential and zig-zag theories. *Journal of Composite Materials*, 2013. doi: 10.1177/0021998313497775.

[59] E. Carrera, G. Giunta, P. Nali, and M. Petrolo. Refined beam elements with arbitrary cross-section geometries. *Computers & structures*, 88(5):283–293, 2010. doi: 10.1016/j.compstruc.2009.11.002.

[60] E. Carrera, A. Pagani, and M. Petrolo. Classical, refined and component-wise analysis of reinforced-shell wing structures. *American Institute of Aeronautics and Astronautics Journal*, 51(5):1255–1267, 213. doi: 10.2514/1.J052331.

[61] E. Carrera, A. Pagani, and M. Petrolo. Component-wise method applied to vibration of wing structures. *Journal of Applied Mechanics*, 80, 2013. doi: 10.1115/1.4007849.

[62] J.F. Davalos, Y. Kim, and E.J. Barbero. Analysis of laminated beams with a layer-wise constant shear theory. *Composite Structures*, 28(3):241 – 253, 1994.

[63] X. Lin and Y.X. Zhang. A novel one-dimensional two-node shear-flexible layered composite beam element. *Finite Elements in Analysis and Design*, 47(7):676 – 682, 2011. doi: 10.1016/j.finel.2011.01.010.

[64] T.P. Vo and H. Thai. Static behavior of composite beams using various refined shear deformation theories. *Composite Structures*, 94(8):2513 – 2522, 2012. doi: 10.1016/j.compstruct.2012.02.010.

[65] M.E. Raville, E.-S. Ueng, and M.-M. Lei. Natural frequencies of vibration of fixed-fixed sandwich beams. *Journal of Applied Mechanics*, 28:367, 1961. doi: 10.1115/1.3641713.

[66] W.P. Howson and A. Zare. Exact dynamic stiffness matrix for flexural vibration of three-layered sandwich beams. *Journal of Sound and Vibration*, 282(3):753–767, 2005. doi: 10.1016/j.jsv.2004.03.045.

[67] J.R. Banerjee, C.W. Cheung, R. Morishima, M. Perera, and J. Njuguna. Free vibration of a three-layered sandwich beam using the dynamic stiffness method and experiment. *International Journal of Solids and Structures*, 44(22):7543–7563, 2007. doi: 10.1016/j.ijsolstr.2007.04.024.

[68] E. A. Armanios and A. M. Badir. Free vibration analysis of anisotropic thin-walled closed-section beams. *AIAA journal*, 33(10):1905–1910, 1995. doi: 10.2514/3.12744.

[69] M. Gunay and T. Timarci. Free vibration of composite box-beams by ansys. In *International Scientific Conference (UNITECH), Gabrovo, Bulgaria*, 2012.

[70] R. Chandra and I. Chopra. Experimental-theoretical investigation of the vibration characteristics of rotating composite box beams. *Journal of Aircraft*, 29(4):657–664, 1992. doi: 10.2514/3.46216.

[71] E. Carrera, M. Filippi, P. K.R. Mahato, and A. Pagani. Advanced models for free vibration analysis of laminated beams with compact and thin-walled open/closed sections. *Journal of Composite Materials*, 2014. doi: 10.1177/0021998314541570.